Imperial College of Science & Technology

ANALYSIS OF TRANSVERSE MOMENTUM AND EVENT SHAPE IN νN SCATTERING

IC/HEP/89/8
October 1989

ANALYSIS OF TRANSVERSE MOMENTUM AND EVENT SHAPE IN νN SCATTERING

Aachen-Birmingham-Bonn-CERN-Demokritos-Imperial College-Munich-Oxford-Saclay-University College Collaboration
(WA21 & WA47)

P. C. BOSETTI, H. GRÄSSLER, D. LANSKE, R. SCHULTE and K. SCHULTZE
III Physikalisches Institut der Technischen Hochschule, Aachen, Germany

G.T. JONES, R.W.L. JONES (*), B.W. KENNEDY and S.W. O'NEALE
Department of Physics, University of Birmingham B15 2TT, U.K.

C. GEICH-GIMBEL, B. NELLEN and B. WÜNSCH
Physikalisches Institut der Universität Bonn, Bonn, Germany

H. KLEIN, D.R.O. MORRISON and H. WACHSMUTH
CERN, European Organization for Nuclear Research, Geneva, Switzerland

E. SIMOPOULOU and A.VAYAKI
Nuclear Research Centre, Demokritos, Athens, Greece

K. W. J. BARNHAM, F. HAMISI, D. B. MILLER, M. M. MOBAYYEN and S. WAINSTEIN
Imperial College of Science , Technology and Medicine, London SW7 2AZ, U.K.

M. ADERHOLZ, D. HANTKE, E. HOFFMANN, U. F. KATZ, J. KERN, N. SCHMITZ and W. WITTEK
Max-Planck-Institut für Physik und Astrophysik, Munich, Germany

C. ALBAJAR, J. R. BATLEY, G. MYATT, D. H. PERKINS, D. RADOJICIC, P. RENTON and B. SAITTA
Department of Nuclear Physics, Oxford OX1 3RH, U.K.

T. BOLOGNESE, J. VELASCO and D. VIGNAUD
Centre d'Etudes Nucleaires, Saclay, France

F.W. BULLOCK and S. BURKE (**)
Department of Physics and Astronomy, University College London, London WC1E 6BT, U.K.

Submitted to Zeitschrift für Physik C

ABSTRACT

The transverse momentum distributions of hadrons produced in neutrino-nucleon charged current interactions and their dependence on W are analysed in detail. It is found that the components of the transverse momentum in the event plane and normal to it increase with W at about the same rate throughout the available W range. A comparison with e^+e^- data is made. Studies of the energy flow and angular distributions in the events classified as planar do not show clear evidence for high energy, wide angle gluon radiation, in contrast to the conclusion of a previous analysis of similar neutrino data.

(*) Now at Queen Mary College, London E1 4NS, U.K.
(**) Now at Rutherford Appleton Laboratory, Chilton, Didcot, Oxon OX11 0QX, U.K.

1. Introduction

The general characteristics of the transverse momentum distribution of charged hadrons produced in inelastic neutrino-nucleon scattering have been described in previous papers, analysing data from charged current events in BEBC filled either with a Ne/H_2 mixture and exposed to the CERN narrow band beam [1], or with H_2 and exposed to the wide band beam [2] or filled with D_2 and exposed to the wide band beam [3]. All experiments detected an increase of $< p_T^2 >$, the average transverse momentum squared of the hadrons in the forward jet, with increasing W, the invariant mass of the hadronic system. This rise is in qualitative agreement with the prediction of QCD based models. The significance of any quantitative comparison is reduced by the assumptions that must be made about the uncalculable non-perturbative contributions. It is therefore important to ascertain whether the data exhibit some features, other than the increase of $< p_T^2 >$ with W, which are typical of hard gluon emission (e.g. planarity, three-jet structure, characteristics of the energy flow shapes).

In this paper an analysis is made of the charged current (CC) events from two BEBC experiments [1,2] which are combined in order to increase the statistical weight of the sample. The full WA21(H_2) and WA47 (Ne/H_2) neutrino data are used. This constitutes a total of 458400 frames of WA21 pictures and 262000 WA47 pictures which yield 51533 and 8055 events respectively.

The paper is divided as follows: section 2 contains experimental details, section 3 describes the p_T^2 distributions, in section 4 the average p_T^2 in and out of the event plane are discussed, sections 5 and 6 deal with planarity distributions and energy flow, and conclusions are summarised in section 7.

2. Experimental Details

Both experiments took place in BEBC exposed to the CERN wide band beam (WA21) or narrow band beam (WA47). The target in the WA21 experiment was H_2 ; the target in the WA47 experiment was 74% mole Ne/H_2 corresponding to a radiation length of ~ 40 cm. A 3.5 T magnetic field was used to measure charged particle momenta; muons were identified by an external muon identifier (EMI) [4]. The BEBC volume was photographed by 4 standard cameras; the film scanning efficiency was typically 95 ± 2% for the events used in this paper.An event is classified as a CC if it has one muon with $p_\mu > 3$ GeV/c, and neutrino energy $E_\nu > 8$ GeV. This leaves a total of 9185 νp and 2576 νNe events.The

measured hadronic energy in each event is corrected by applying a suitable factor based on transverse momentum balance [5]. The incident neutrino energy, E_ν , is taken as the sum of the muon and corrected hadronic energies. Q^2, the four momentum transfer squared, and W^2 are computed from E_ν and the muon momentum p_μ. The events are further selected by applying the cuts $W > 4$ GeV and $Q^2 > 1$ GeV^2 . These cuts, together with a minimum multiplicity of 3 charged hadrons, leave 5938 νp and 2157 νNe events. In part of the analysis the more severe restriction of demanding at least 3 charged forward hadrons is applied, which further reduces the sample to 4670 events in total. The analysis is restricted to the charged hadrons only. In the neon experiment, identified protons of momentum less than 300 MeV/c, associated with nuclear break-up, are excluded.

The 'jet-axis' with respect to which p_T is evaluated can be defined in the following ways :

(a) the resultant momentum vector $\vec{q}_H$ of the visible hadrons in the lab system;

(b) the current vector $\vec{q}_c$ computed from the corrected neutrino energy and muon momentum;

(c) the sphericity axis $\vec{s}$, i.e. the direction which minimises $\Sigma\, p_T^2$ (sum over the visible charged hadrons in the hadronic centre of mass system).

p_T is defined as the transverse momentum of a particle with respect to one of the above axes. For $W > 4$ GeV and $Q^2 > 1$ GeV^2 these directions are close to one another. For example, the mean angle between $\vec{q}_c$ and $\vec{q}_H$ is ~ 2° and between $\vec{q}_c$ and $\vec{s}$ is ~ 15° in the laboratory frame.

In what follows we use a system of orthonormal axes $\vec{n}_1$, $\vec{n}_2$, $\vec{n}_3$ defined so that $\vec{n}_3$ coincides with the jet axis and $\vec{n}_2$ is chosen to maximise

$$\sum_j (\vec{p}_j \cdot \vec{n}_2)^2$$

for the measured hadrons of the event. The vectors $\vec{n}_2$ and $\vec{n}_3$ define the 'event plane', with $\vec{n}_1$ perpendicular to it.

Forward hadrons in this analysis are defined as those with $x_F > 0$, where

$$x_F = \frac{2p_l}{W}$$

and p_l is the component of momentum along the $\vec{q}_H$ axis in the centre of mass system of the visible hadrons. All unidentified hadrons (essentially those with $p > 1$ GeV/c in the laboratory frame) are assumed to be pions. Particles with a momentum error of more than 30% have been excluded, and when such a particle carries more than 30% of the total hadronic energy the event is rejected. This constitutes 2% of all tracks and 8.5% of all events respectively.

3. p_T^2 Distributions and their W Dependence

In Fig. 1 the p_T^2 distributions

$$\frac{1}{N_h} \cdot \frac{dN_h}{dp_T^2}$$

(p_T relative to $\vec{q}_H$ axis) of forward (a) and backward (b) going hadrons are shown for hydrogen and neon targets and for two different W ranges. The distribution for $x_F > 0$ shows a significant W dependence at higher p_T ($p_T \geq 1$ GeV/c). The size of the effect caused by the choice of the jet axis is illustrated in Fig. 1(c) and (d), where the p_T^2 distributions, for forward hadrons only, with respect to the $\vec{q}_H$ and $\vec{s}$ axes are compared. The minimisation procedure for $\vec{s}$ tends to suppress the high p_T tail of the p_T distribution (Figs. 1c and 1d). Since the sphericity axis is the only axis available for e^+e^- annihilation data we have used $\vec{s}$ to compare with e^+e^-, whereas $\vec{q}_H$ is chosen for the main analysis of this paper.

The W dependence, observed in the forward direction, is mainly associated with particles of large x_F. This is illustrated in Fig. 2, which shows $< p_T^2 >$ (relative to $\vec{q}_H$) as a function of x_F for different W ranges. The $< p_T^2 >$ of backward going hadrons does not have a strong dependence on W, while that of the forward hadrons increases significantly at high W and x_F.

This asymmetry, in agreement with results of the other neutrino experiments [6,7], is qualitatively consistent with the notion that the forward scattered quark is strongly accelerated and is therefore expected to radiate gluons, thus broadening the forward p_T^2 distribution, whereas for the spectator diquark the effects are

expected to be small. Fig. 3 shows $< p_T^2 >$ versus W^2 for $x_F > 0.05$ (a) and $-0.7 < x_F < -0.05$ (b). This is directly comparable and in good agreement with the data of ref. [7].

For particles travelling forward in the hadronic c.m.s., in events with $W < 8$ GeV, the p_T^2 distribution, using $\vec{q}_H$ as an axis, is reasonably well described throughout the whole p_T^2 range by the expression :

$$\frac{1}{N_h}\frac{dN_h}{dp_T^2} = Ae^{-bm_T}, \qquad (1)$$

with $m^2_T = p_T^2 + m_\pi^2$ and $b \sim 5.5\ GeV^{-1}c^2$. This parameterisation is used later in a Monte Carlo generation of events which are compared with the data.

In this section the data from Ne and H_2 experiments have been shown as distinct points to demonstrate that there is agreement (at least as far as transverse momentum is concerned) between the two experiments, and therefore it is justified to combine the two samples.

4. p_T In and Out of the Event Plane

The general trend of the p_T^2 distributions and their W dependence agrees well with other neutrino experiments [6,7], and is similar to that found in e^+e^- annihilation at PETRA [8,9,10] as well as in hadron-hadron collision [11] and in inelastic μp scattering [12]. As explained above we use the $\vec{s}$ axis to compare our data with the results of e^+e^- annihilation in spite of the resulting systematic reduction of p_T. To allow for different detection efficiencies in the neutrino and e^+e^- experiments, in the neutrino data we have removed particles with momentum less than 300 MeV/c in the centre of mass system of the visible hadrons and rejected events with less than 4 charged hadrons. For $W > 6$ GeV these cuts leave the results essentially unaltered.

For a selected set of events we define the average $< p_T^2 >_{IN}$ and $< p_T^2 >_{OUT}$ of hadrons in and out of the event plane as :

$$< p_T^2 >_{IN} = \frac{1}{N_h}\sum_{j=1}^{N_h} (\vec{p}_j \cdot \vec{n}_2)^2 \qquad (2)$$

$$< p_T^2 >_{OUT} = \frac{1}{N_h} \sum_{j=1}^{N_h} (\vec{p}_j . \vec{n}_1)^2 \qquad (3)$$

where N_h is the total number of charged hadrons in the hemisphere considered (forward or backward) in all the events passing the selection requirements.
Fig. 4 shows these averages as functions of W^2 with $x_F > 0$, using $\vec{q}_H$ or $\vec{s}$ as the event axes. Obviously $< p_T^2 >_{IN}$ is greater than $< p_T^2 >_{OUT}$ by definition. In Fig. 4 the neutrino data (representing the total of hydrogen and neon events with W> 4 GeV and $Q^2 > 1 GeV^2$) are compared with e^+e^- data from the TASSO, PLUTO and JADE experiments [8,9,10]*. The difference due to the choice of event axis (which affects the magnitude of $< p_T^2 >_{IN}$ and $< p_T^2 >_{OUT}$ much more than the W dependence in the neutrino data) is of the same order as the apparent discrepancy between different e^+e^- experiments. This makes a quantitative comparison difficult, although the neutrino data, with $\vec{s}$ as event axis, should be directly comparable with the e^+e^- results. The trend of the W dependence of both $< p_T^2 >_{IN}$ and $< p_T^2 >_{OUT}$ in e^+e^- annihilation and in the forward hemisphere in νN scattering (Fig. 4) is similar and shows, at least in the W range spanned by the neutrino data, about the same rate of increase.
We will not investigate the details of p_T^2 dependence in this paper, this has already been done for example in refs[2,3] . But we note that this has been understood in concepts such primordial p_T , soft and hard gluon emission as in refs [8,9,10].
We note that single hard gluon emission in this kinematic region is expected to be a rare process.
However three-jet hadron structures have been reported in an experiment [7] similar to ours, so we examine our data to search for possible hard gluon processes.
In the course of this search, in order to distinguish new dynamical effects from those that are simply due to kinematical or trivial constraints, we compare the data with two Monte Carlos, a longitudinal phase space (LPS) Monte Carlo and a QCD based Monte Carlo (LUND).
The LPS has all kinematics built in but has no dynamical effects. Each event was generated according to the known neutrino flux distribution. The scaling variables Bjorken x and y were generated from a Q^2 dependent

---

* It should be noted that these average values have been computed from published histograms, and do not include tails in the distributions if they are not shown.

parameterisation of quarks and gluons. The total charged and neutral multiplicities were chosen from a Poisson distribution with a mean value proportional to ln (W^2). The mesons were generated as charged and neutral particles with the mean number of neutrals approximately half that of the charged mesons. The transverse momenta of all particles were chosen from a distribution of e^{-bm_T} where $m_T = \sqrt{m^2 + p_T^2}$ with $b = 5.5\ (GeV)^{-1}$ obtained from fits to the p_T distribution of neutrino events. Each meson was assigned a rapidity according to a flat distribution over the kinematically allowed range given by W. Instrumental effects were then added by smearing the measured variables.
The LUND Lepto production model is used for the QCD based Monte Carlo. The model used a first order α_s contribution giving rise to qg and $q\bar{q}$ events [14]. The QCD parameters were set to $\Lambda = 400$ MeV, $\langle k_T \rangle = 420$ MeV and $\alpha_s = 0.26$. Again instrumental effects were added by appropriate smearing of measured variables. The ratio

$$R = \frac{\langle p_T^2 \rangle_{IN}}{\langle p_T^2 \rangle_{OUT}} \qquad (4)$$

for the forward (a) and backward (b) hemispheres, using $\vec{q}_H$ as event axis, is shown as a function of W^2 in Fig. 5. If hadrons were produced with azimuthal isotropy about the jet axis this ratio would fall slowly and monotonically with W, because of the logarithmic rise of the average multiplicity. The minimum charged multiplicity imposed by our selection, however, has the effect of reducing the value of R, especially at low W. Since both LPS and LUND Monte Carlos agree well with the data we see no evidence for hard gluon effects, so search for further selections to isolate events with possible hard gluon emission.

5. Planar Events

In this section we will consider the features of the data which have been claimed [7] to constitute evidence for hard gluon radiation. The data are consistent with the bulk of the events being two-jet like as one might have expected, since the fraction of events where a single hard gluon has been radiated is expected to be small. However, there could still be a class of events, with characteristics different from the rest, which could be attributed to a first order QCD process, as claimed by BFHSW [7]. Characteristics typical of hard gluon emission are a "planar" structure of the event, connected with a 3-body (e.g. quark-gluon-diquark) origin of the hadrons, and a larger spread in transverse momentum, especially in the

hemisphere containing the radiated gluon, which in our case is more likely to be the forward rather than the backward c.m.s. hemisphere.

To search for such events, we determine (following ref. [7]) two quantities for each event, namely the planarity

$$P = \frac{\sum (p_T^2)_{IN} - \sum (p_T^2)_{OUT}}{\sum (p_T^2)_{IN} + \sum (p_T^2)_{OUT}}, \qquad (5)$$

and the dispersion in the transverse momentum

$$\Pi = \frac{1}{\sqrt{N_F}} \sum_{1}^{N_F} (p_T - < p_T >) \qquad (6)$$

where $< p_T >$ is the average absolute transverse momentum of the forward hadrons (with respect to the $\vec{q}_H$ axis), averaged over all events, and N_F is the number of forward hadrons in each event. P is computed using all charged hadrons in the event, while Π uses only the forward hadrons. The distribution in Π is approximately gaussian ($< \Pi > \sim 0$, $\sigma \sim 0.2$ GeV/c) with a tail towards high Π values.

Fig. 6 shows the planarity distribution in $1/N_{ev}\ dN_{ev}/dP$ for three separate selections of events; for all events with $N_F \geq 3$; for events with at least one forward hadron having $p_T > 1$ GeV/c ; and for events which have in addition a large spread in transverse momentum ($\Pi > < \Pi > + 2\sigma$). The planarity distributions from this experiment agree well with those obtained in ref. [7] when the same cuts are used. To enable a direct comparison we show in Fig. 7 $1/N_{ev}\ dN_{ev}/dP$ for $W^2 > 50$ GeV^2 and $Q^2 > 2$ GeV^2. It should be noted that with these cuts our event sample is larger than that of ref. [7]. Also shown is the planarity distribution for events with $\Pi > 0.75$, which is equivalent to the requirement $\Pi > 3$ of ref. [7] once the different constant in the definition of Π (eq. 6) is taken into account.

Fig. 6 shows that there is a correlation between P and a large spread in transverse momentum and a stronger correlation between P and the presence of a high p_T track in the data. Neither the requirement of a high p_T track (dot-dashed line in Fig. 6) nor the requirement of high dispersion in transverse momentum

(dashed line in Fig. 6) applied to the LPS Monte Carlo reproduces the data well, although small enhancements are seen at high P.

The LPS Monte Carlo does not reproduce the correct shape and fraction of 'planar events' (see table 1) which have a large spread in transverse momenta. The data are more planar. The p_T distribution in the LPS Monte Carlo ($e^{-5.5m_T}$) also fails to reproduce the high p_T component present in the data at high W. (However section 6 shows that the energy flow is well reproduced by the LPS Monte Carlo).

6. Analysis of Planar Events

As described in section 5, a planar event most commonly results from the emission of one (or more) hadrons of exceptionally large p_T. In what follows we investigate in detail the properties of the subsample of events for which at least one forward hadron has $p_T > 1$ GeV/c.

The study of angular energy flow enables the experimental data to be compared with QCD predictions which are infrared safe [16] and do not depend on the form assumed for the fragmentation function, this being achieved by means of z-weighting.

The angular energy flow is defined as

$$\frac{d\Sigma}{d\theta} = \frac{1}{N_{ev}} \frac{\sum_{j=1}^{N_h} z_j}{\Delta\theta}, \qquad (7)$$

where N_h is the number of hadrons in the angular interval $\Delta\theta$, θ being the angle between the jet axis, $\vec{q}_H$ axis, and the momentum vector of a particular hadron projected into the ($\vec{n}_3$, $\vec{n}_2$) plane (i.e. the event plane) in the centre of mass of the visible hadrons. z_j is here defined as $2E_j$ (cms) / W.

Fig. 8 shows the angular energy flow for events with at least three charged forward hadrons and with at least one forward hadron with $p_T > 1$ GeV/c. Due to the different proton detection efficiencies in the hydrogen and neon experiments all identified protons have been excluded from this plot.

The angular energy flow shows a pronounced dip at small angles in the forward direction. This experimental result is in qualitative agreement with the results of a similar analysis by the BFHSW collaboration [7]; for completeness in Fig. 9 we show our data with event selection criteria identical to those of ref. [7]

together with the data points of ref. [7]. It should be noted that neutral hadrons included for the events of ref. [7] have not been included in this analysis. We have checked with samples of our data (WA47) that this introduces no systematic differences, and indeed the data points from ref. [7] and this experiment agree in fig. 9. Note that this experiment has substantially smaller statistical errors.

The LPS Monte Carlo (dashed line) qualitatively reproduces this forward dip. One concludes that the requirement of one particle at high p_T automatically introduces a 'hole' in the forward direction.

Since this apparent three-jet structure can be reproduced solely by the experimental selections on the LPS Monte Carlo events, we disagree with the necessity for hard gluon bremsstrahlung as claimed by ref. [7]. The absence of hard gluon effects at this low W is in agreement with results from e^+e^- annihilation experiments.

7. Conclusion

From an analysis of transverse momenta of final state hadrons produced in νp and νNe interactions, the following conclusions can be drawn:
A rise in $< p_T^2 >$ as a function of W^2 is observed and is mainly associated with forward hadrons carrying a large fraction of the energy. For the forward going hadrons the values of $< p_T^2 >_{IN}$ and $< p_T^2 >_{OUT}$ increase with W^2 at about the same rate. These results show that the bulk of the hadrons are not emitted preferentially in one plane, as might be expected if the increase were due to single hard gluon emission at wide angle. Studies using backward going hadrons and also using Monte Carlo simulated events indicate that the limited multiplicity reduces the sensitivity of this type of analysis to planar effects.

Futher searches for a sample of three-jet events, along the lines suggested by ref. [7] finds three-jet structures in the energy flow, in agreement with the results of [7]. However the same structures are also produced from our LPS Monte Carlo and so they cannot be due to hard gluon effects but must be accidental artfacts of the selection criteria used.

Acknowledgements
We wish to acknowledge the support of the SPS and BEBC crews and the scanning and programming staff in each of the collaborating laboratories.

REFERENCES

1) P.C. Bosetti et al., Nucl. Phys. **B 149** (1979) 13
H. Deden et al., Nucl. Phys. **B 181** (1981) 375

2) P. Allen et al., Nucl. Phys. **B 188** (1981) 1
G.T. Jones et al., Z. Phys. **C 25** (1984) 121

3) D. Allasia et al., Z. Phys. **C 27** (1985) 239

4) R. Beuselinck et al., Nucl. Inst. Meth. **154** (1978) 445

5) H.G. Heilmann, Bonn Internal Report (1978) WA21-Int-1

6) T. Kitagaki et al., Phys. Lett. **97 B** (1980) 325

7) H.C. Ballagh et al., Phys. Rev. Lett. **47** (1981) 556

8) R. Brandelik et al., Phys. Lett. **86 B** (1979) 243
M. Althoff et al., Z. Phys. **C 22** (1984) 307

9) Ch. Berger et al., Phys. Lett. **86 B** (1979) 418
Ch. Berger et al., Z. Phys. **C 22** (1984) 103

10) D.P. Barber et al., Phys. Rev. Lett. **43** (1979) 830
W. Bartel et al., Phys. Lett. **91 B** (1980) 142
G.Wolf, DESY Report (80) 85

11) R. Göttgens et al., Nucl. Phys. **B 178** (1981) 392
M. Barth et al., Z. Phys. **C 22** (1984) 1
D.H. Brick et al., Z. Phys. **C 24** (1984) 19

12) J.J. Aubert et al., Phys. Lett. **95 B** (1980) 306
M. Arneodo et al., Z. Phys. **C 35** (1987) 417
M. Arneodo et al., Phys. Lett. **149 B** (1984) 415

13) G. Ingelman and T. Sjostrand, LUTP 80-12
B. Andersson et al., Phys. Rep. **97** (1983) 31
T. Sjostrand, Comp. Phys. course **27** (1982) 243

14) B. Andersson, G. Gustafson and C. Peterson Z Phys. **C1** (1979) 105
B. Andersson, and G. Gustafson, Z Phys. **C3** (1980) 22

15) J. Kogut and L. Susskind, Phys. Rev. **D 9** (1974) 697

16) A. Mendez, Nucl. Phys. **B 145** (1978) 199
R.D. Peccei and R.Rückl, Nucl. Phys. **B 162** (1980) 125

TABLE CAPTION

Comparison of the fraction of data and LPS Monte Carlo events selected by high dispersion or the presence of a high p_T track. The Monte Carlo reproduces the main features of the data, but not the details of the fractions of high P and $p_T > 1$ GeV/c selections.

(100% = all events selected with W> 4GeV, $Q^2 > 1 GeV^2$ and $N_F \geq 3$).

$W > 4GeV$, $Q > 1GeV^2$ and $N_F \geq 3$

	$\Pi > < \Pi > + 2\sigma$		$p_T > 1$ GeV/c	
	Data	LPS Monte Carlo	Data	LPS Monte Carlo
All Events	2.8% ± 0.2%	2.9% ± 0.1%	4.6% ± 0.2%	3.2% ± 0.1%
Events with P> 0.6	1.3% ± 0.1%	0.7% ± 0.1%	3.2% ± 0.2%	2.1% ± 0.1%

TABLE 1

FIGURE CAPTIONS

1. p_T^2 distributions: (a) and (b) are p_T relative to $\vec{q}_H$ for forward and backward hadrons respectively; (c) and (d) show the influence of using the $\vec{s}$ axis instead of $\vec{q}_H$ for forward hadrons in hydrogen and neon respectively.

   The meanings of the symbols are : open symbols are for H_2, filled symbols are for Neon data,
   ○ ● are for $4 < W < 7$ GeV, △ ▲ are $W > 7$ GeV, all for p_T with respect to the $\vec{q}$ axis; □ ■ are $W > 7$ GeV for p_T with respect to the $\vec{s}$ axis.

2. $< p_T^2 >$ as a function of x_F for different W ranges for Ne and H_2 separately. p_T is measured relative to the $\vec{q}_H$ axis.

3. $< p_T^2 >$ as a function of W^2 for forward (a) and backward (b) hadrons for Ne and H_2 separately. p_T is measured relative to the $\vec{q}_H$ axis.

4. $< p_T^2 >_{IN}$ and $< p_T^2 >_{OUT}$ relative to $\vec{q}_H$ and $\vec{s}$ for forward hadrons as a function of W^2. Results from e^+e^- annihlations are included for comparison.

5. The ratio R for forward (a) and backward (b) hemispheres as a function of W^2. Lund and LPS Monte Carlo data are also shown.

6. The planarity distributions for (i) all events with $N_F \geq 3$ (histogram), (ii) $N_F \geq 3$ and at least one hadron with $p_T > 1$ GeV/c (□ = data, — · — · — · = LPS) and (iii) $N_F \geq 3$ and high dispersion, i.e. $\Pi > < \Pi > + 2\sigma$ (■ = data, — — — = LPS).

7. The planarity distributions for this experiment and the data of reference [7], using the Q^2 and W^2 cut of reference [7] (i.e. $W^2 > 50$ GeV^2 and $Q^2 > 2$ GeV^2). Note that $\Pi = 0.75$ GeV/c here corresponds to $\Pi = 3.0$ in reference [7].

8. The angular energy flow distribution of events with $N_F \geq 3$ and at least one forward hadron with $p_T > 1$ GeV/c. The dashed line shows LPS Monte Carlo data with the same cuts.

9. The angular energy flow as in figure 8 with additional cuts used in reference [7]. ($W^2 > 50$ GeV^2, $Q^2 > 2$ GeV^2, $\Pi > 0.75$ GeV/c $P > 0.5$). Data from reference [7] and the LPS Monte Carlo are included for comparison.

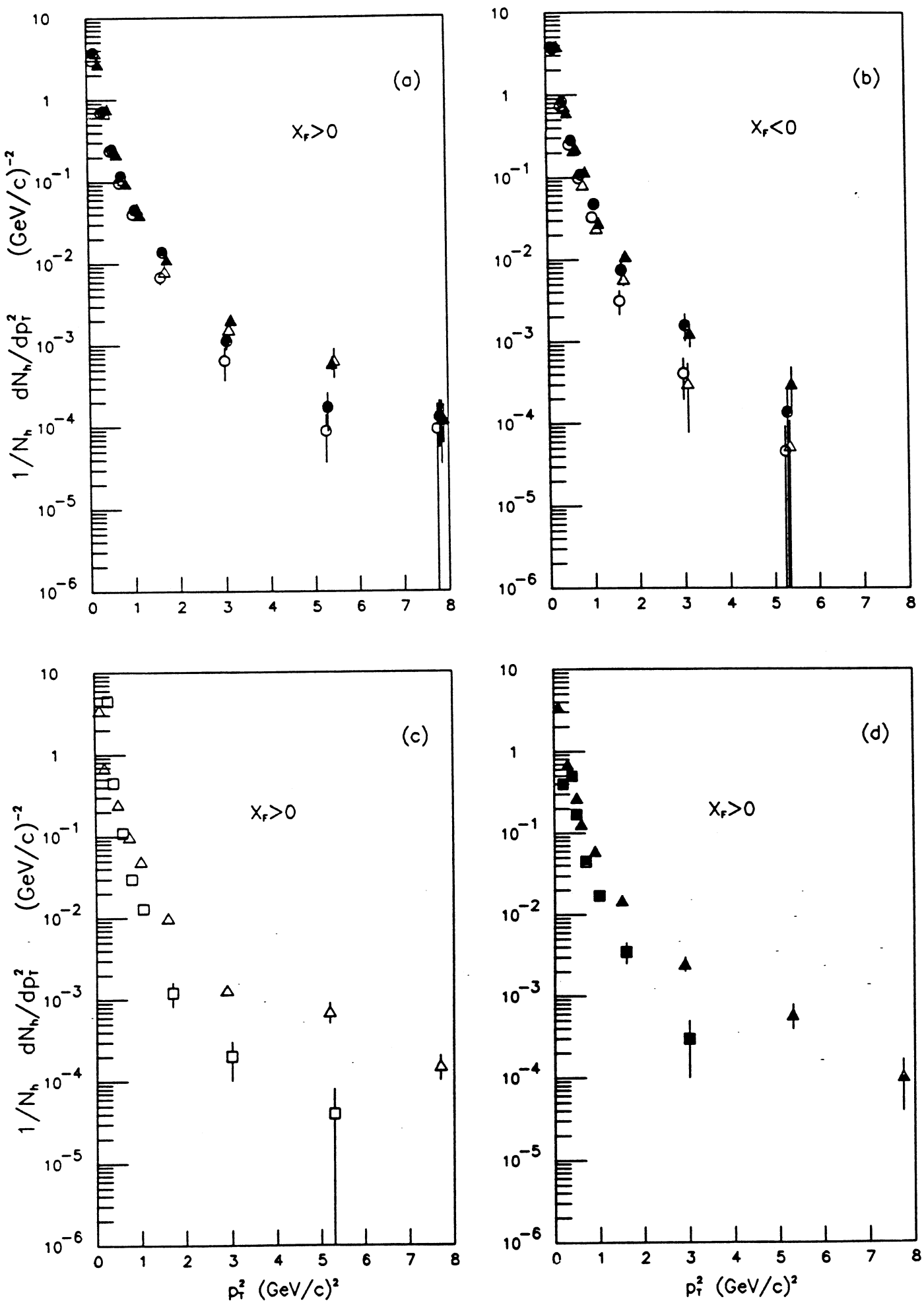

Figure 1

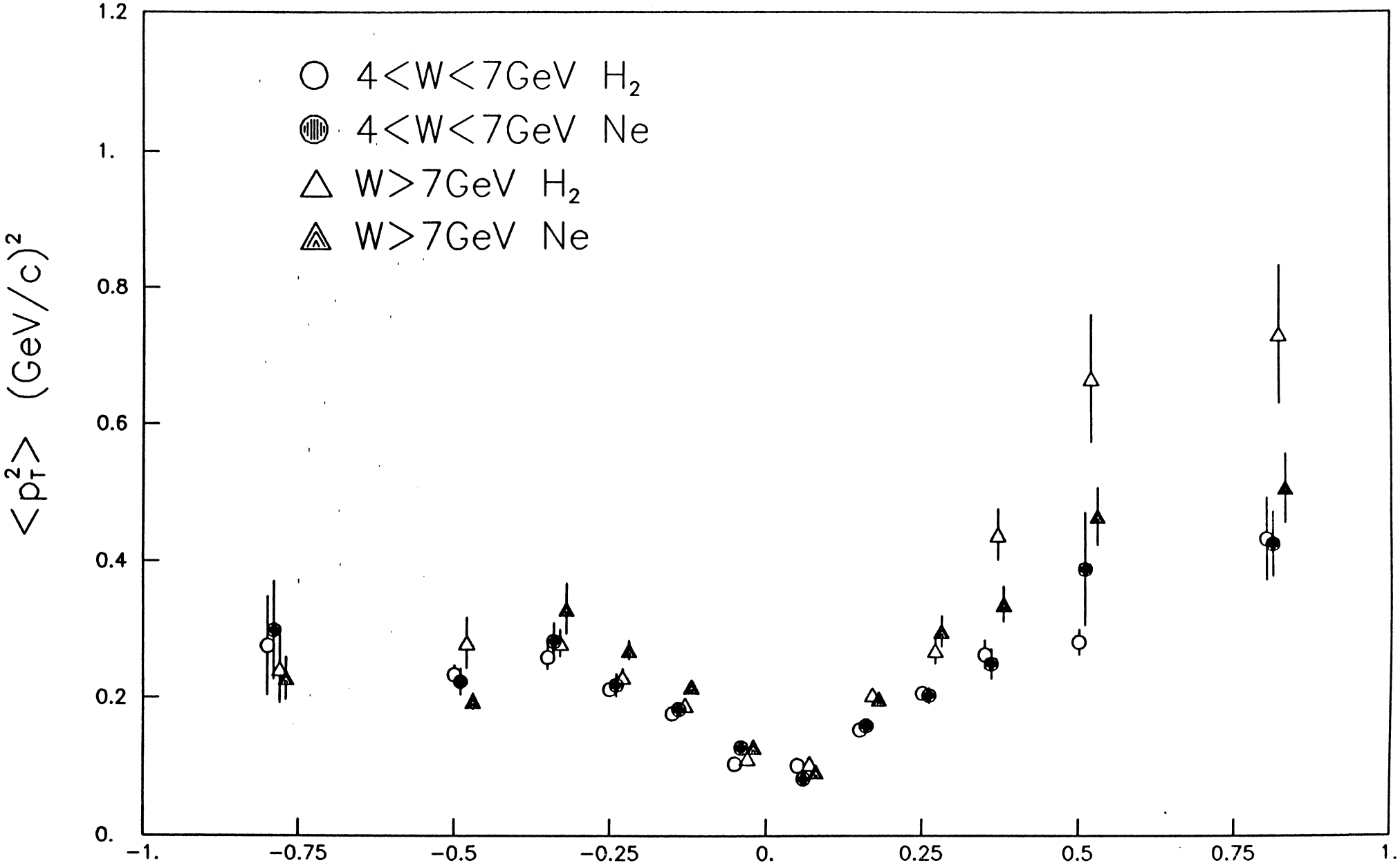
4<W<7GeV H2
4<W<7GeV Ne
W>7GeV H2
W>7GeV Ne
<pT2> (GeV/c)2
1.2
1.
0.8
0.6
0.4
0.2
0.
-1.
-0.75
-0.5
-0.25
0.
0.25
0.5
0.75
1.
XF

Figure 2

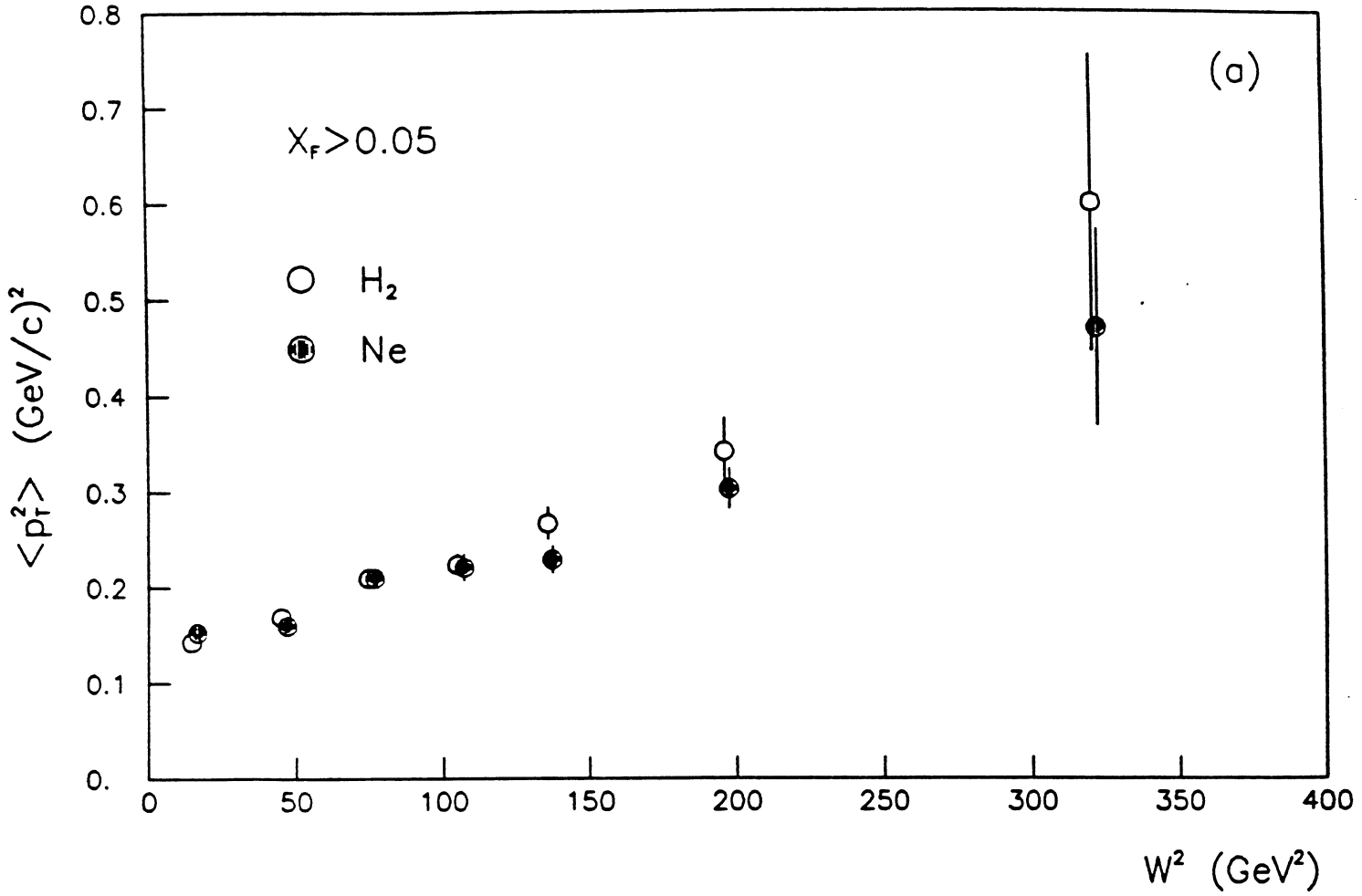
(a)
$X_F > 0.05$
H_2
Ne
$\langle p_T^2 \rangle$ (GeV/c)^2
W^2 (GeV^2)
0.
0.1
0.2
0.3
0.4
0.5
0.6
0.7
0.8
0
50
100
150
200
250
300
350
400

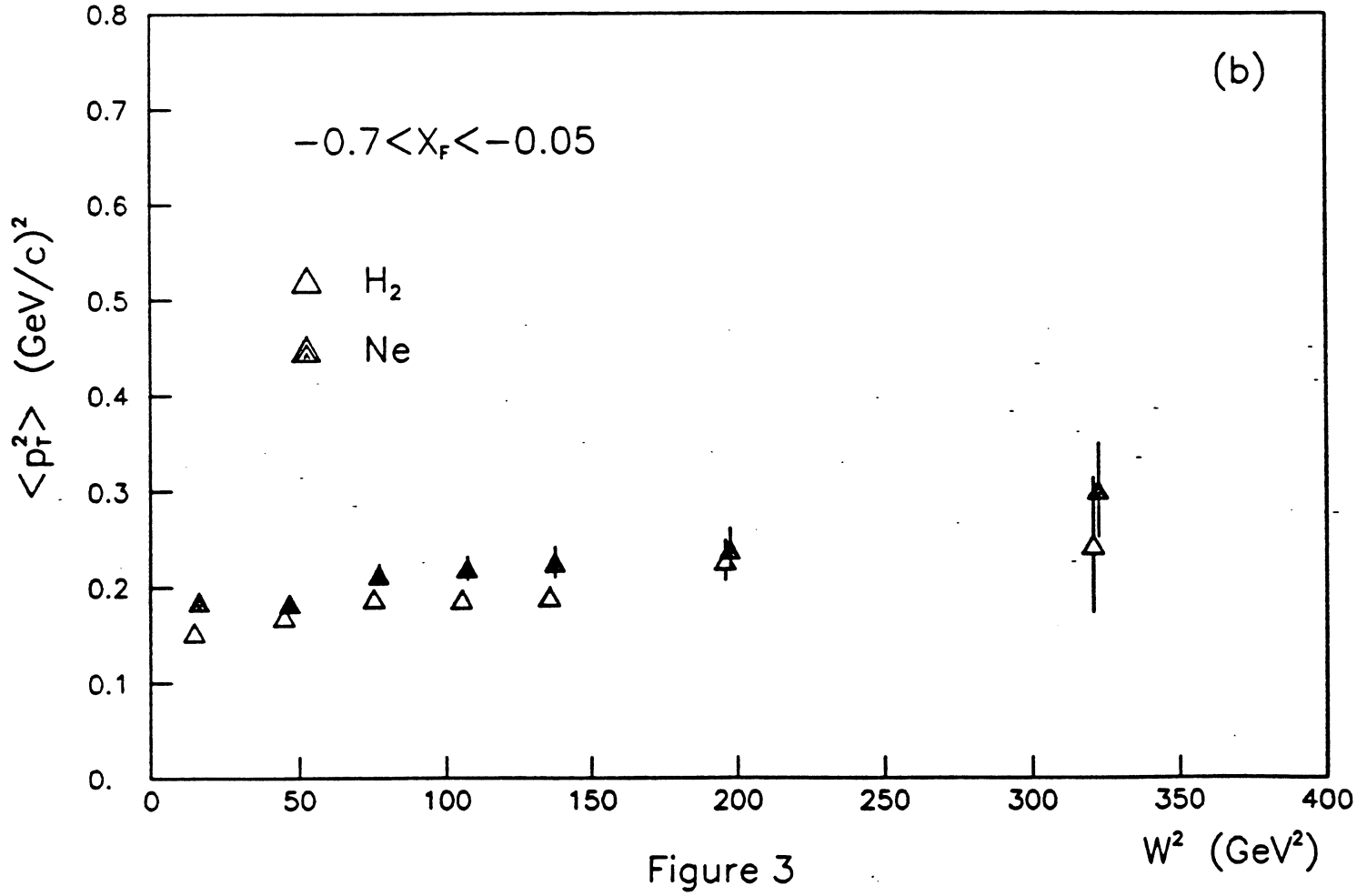
(b)
$-0.7 < X_F < -0.05$
H_2
Ne
$\langle p_T^2 \rangle$ (GeV/c)^2
W^2 (GeV^2)
0.
0.1
0.2
0.3
0.4
0.5
0.6
0.7
0.8
0
50
100
150
200
250
300
350
400

Figure 3

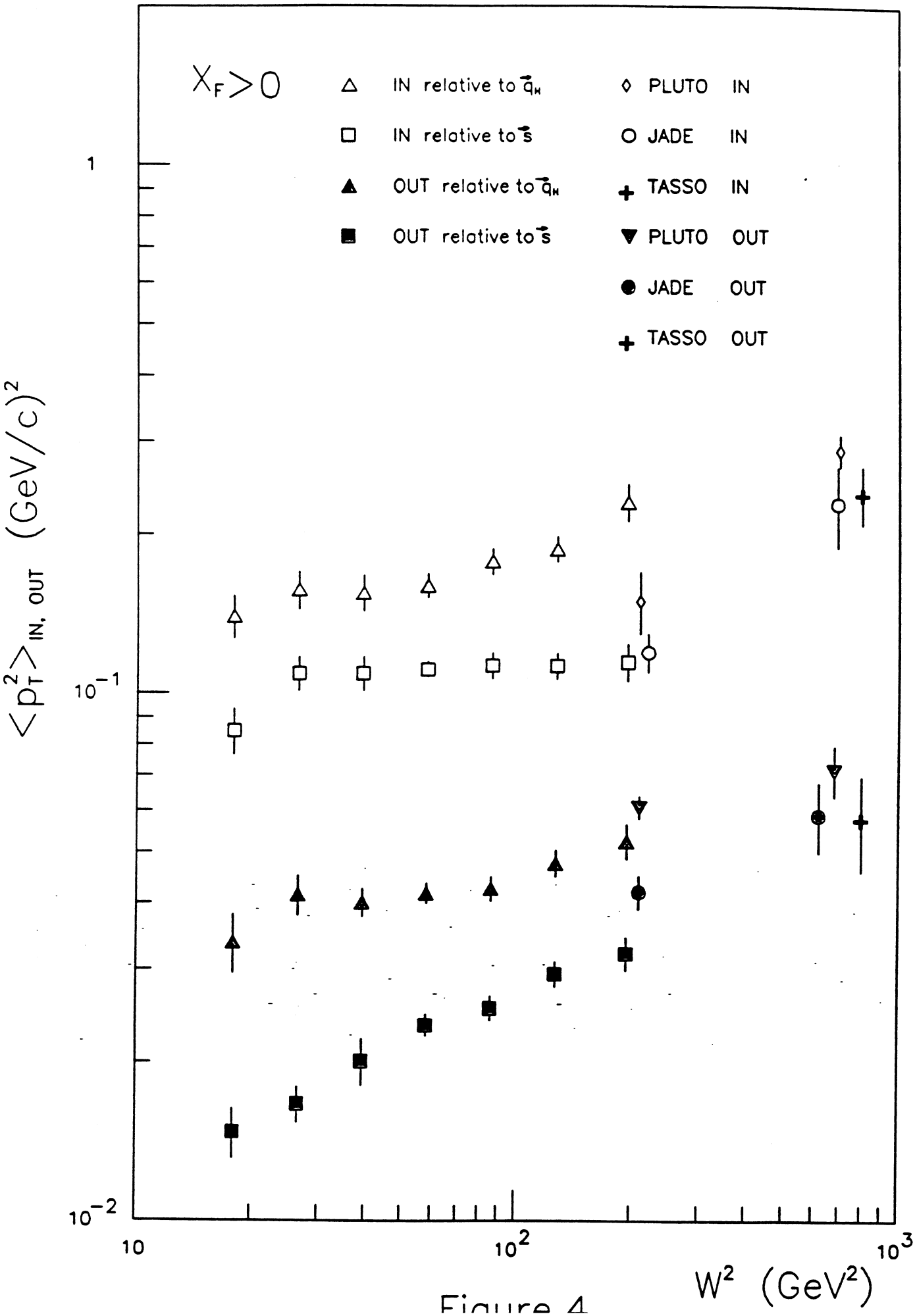
$X_F > 0$
IN relative to $\vec{q}_H$
IN relative to $\vec{s}$
OUT relative to $\vec{q}_H$
OUT relative to $\vec{s}$
PLUTO IN
JADE IN
TASSO IN
PLUTO OUT
JADE OUT
TASSO OUT
$\langle p_T^2 \rangle_{IN,\ OUT}$ (GeV/c)^2
1
10^{-1}
10^{-2}
10
10^2
10^3
W^2 (GeV^2)

Figure 4

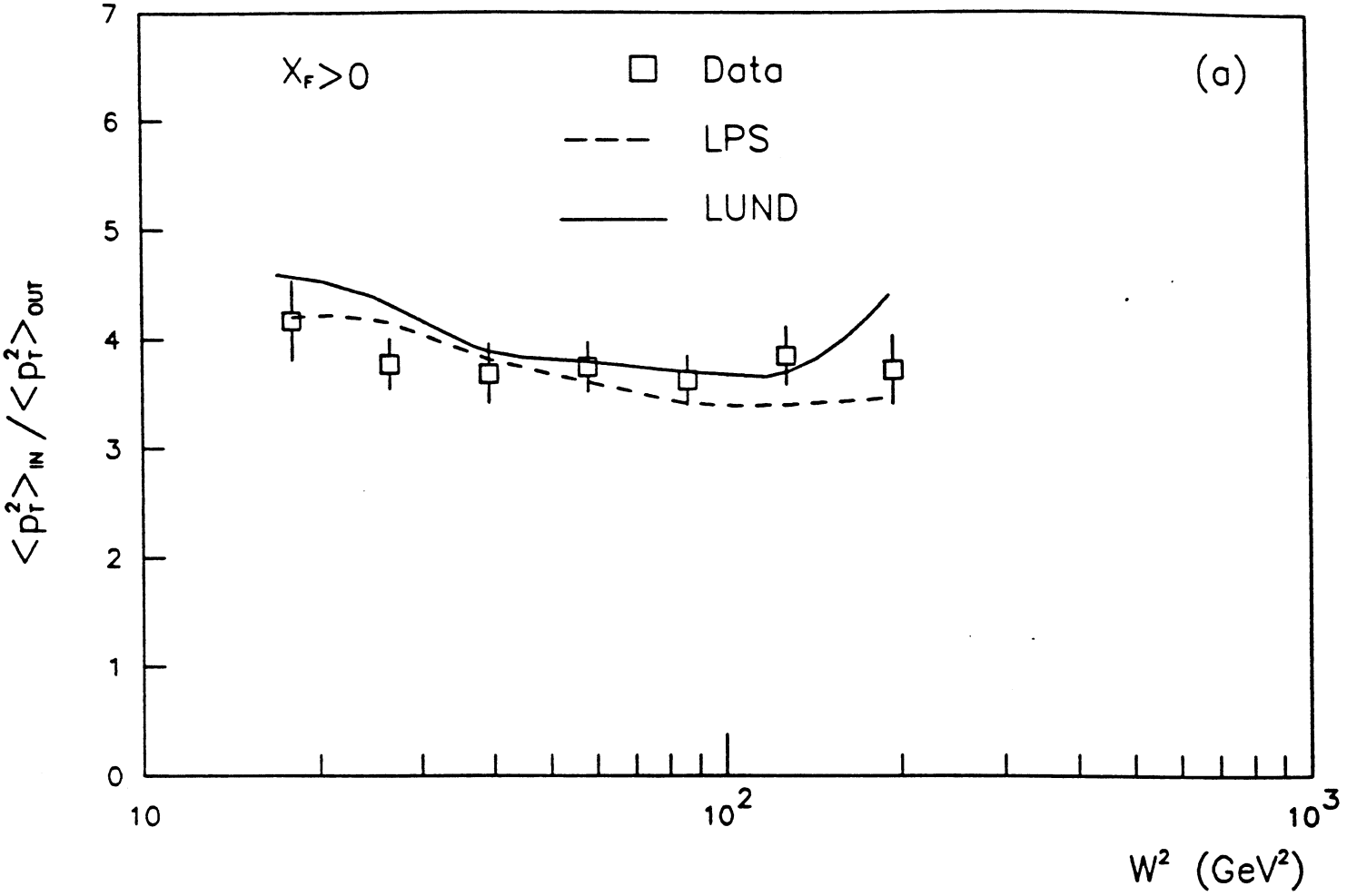
$X_F>0$
Data
LPS
LUND
(a)
$\langle p_T^2\rangle_{IN} / \langle p_T^2\rangle_{OUT}$
W^2 (GeV^2)

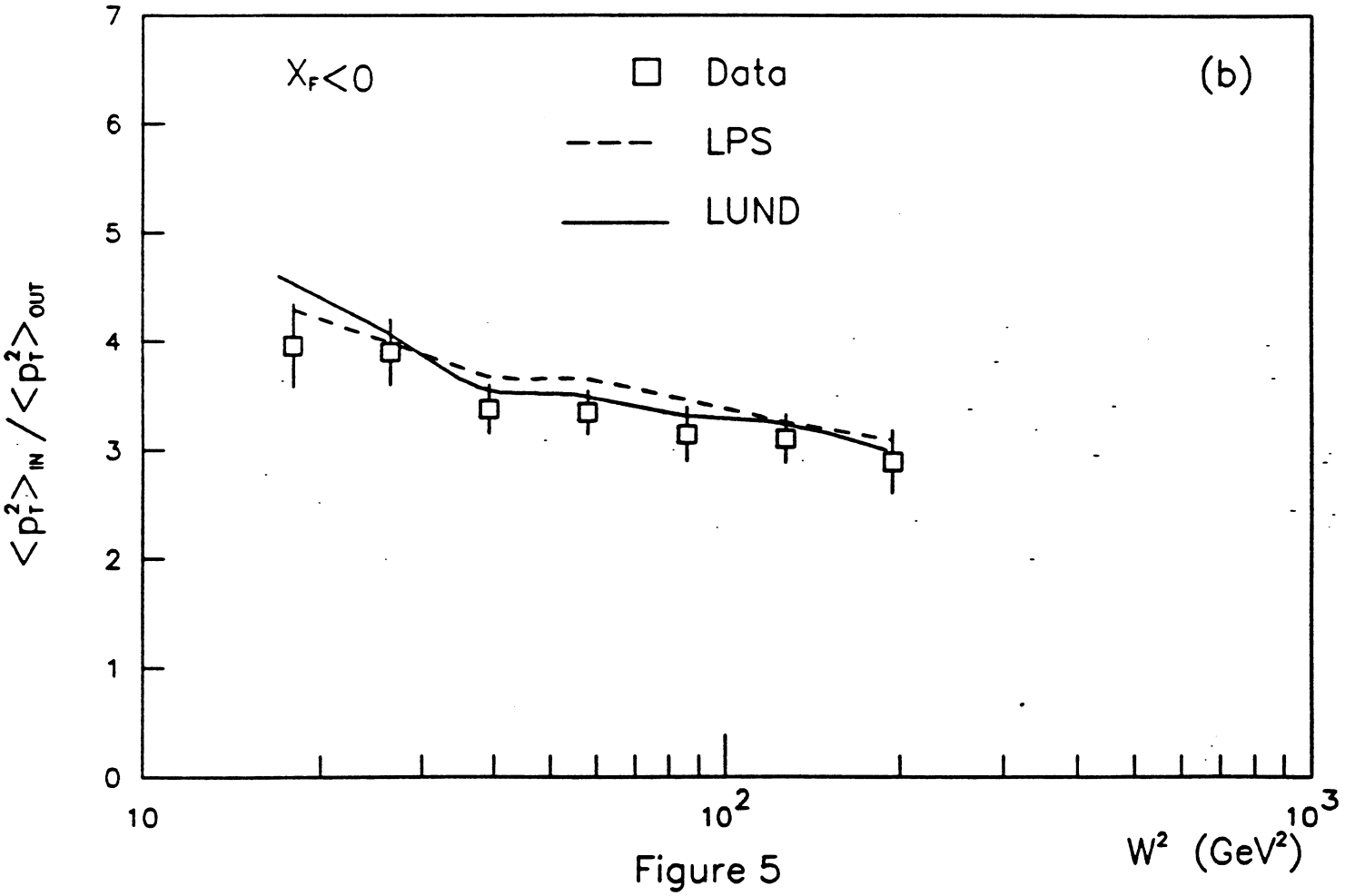
$X_F<0$
Data
LPS
LUND
(b)
$\langle p_T^2\rangle_{IN} / \langle p_T^2\rangle_{OUT}$
W^2 (GeV^2)

Figure 5

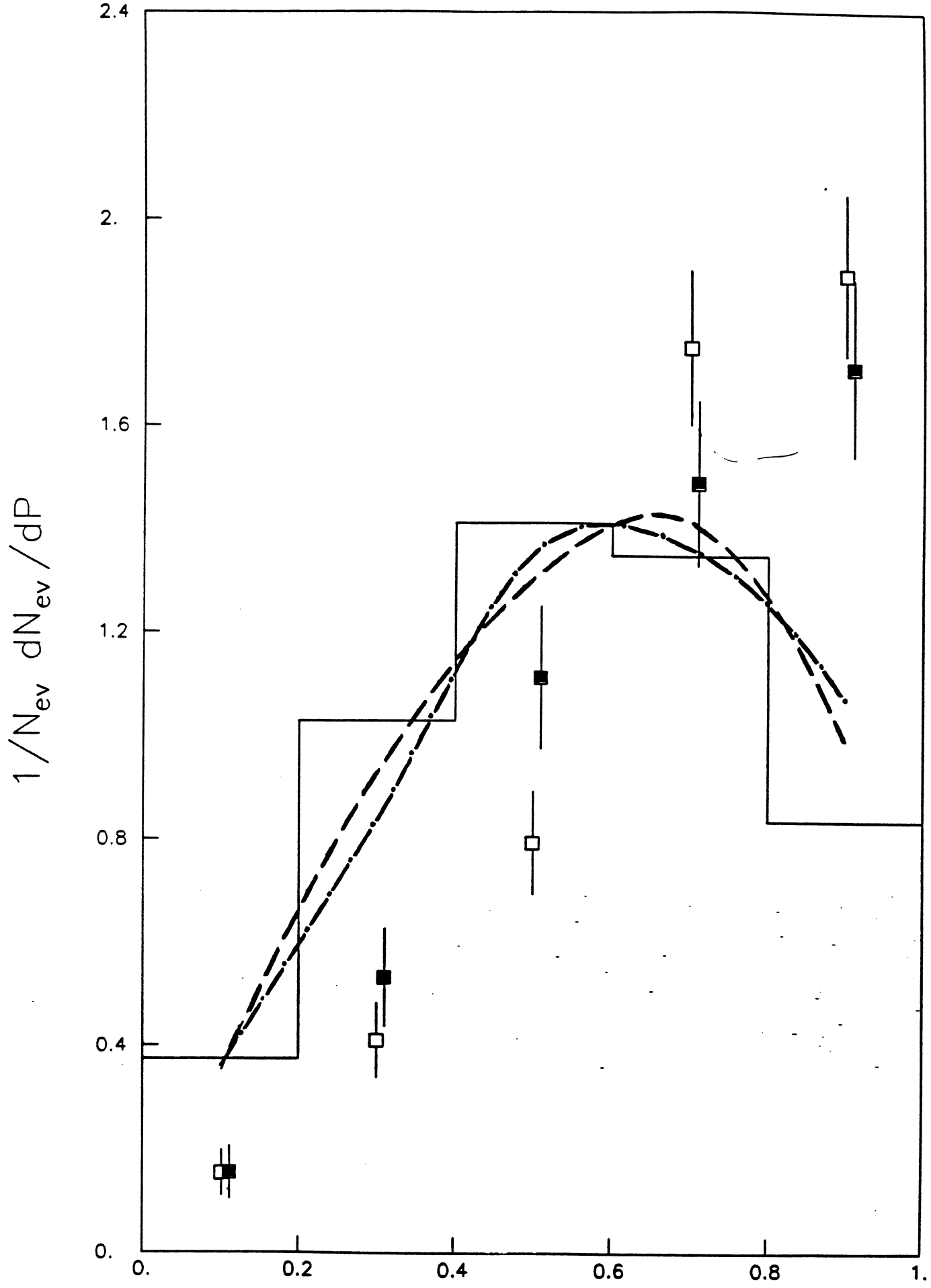

Figure 6

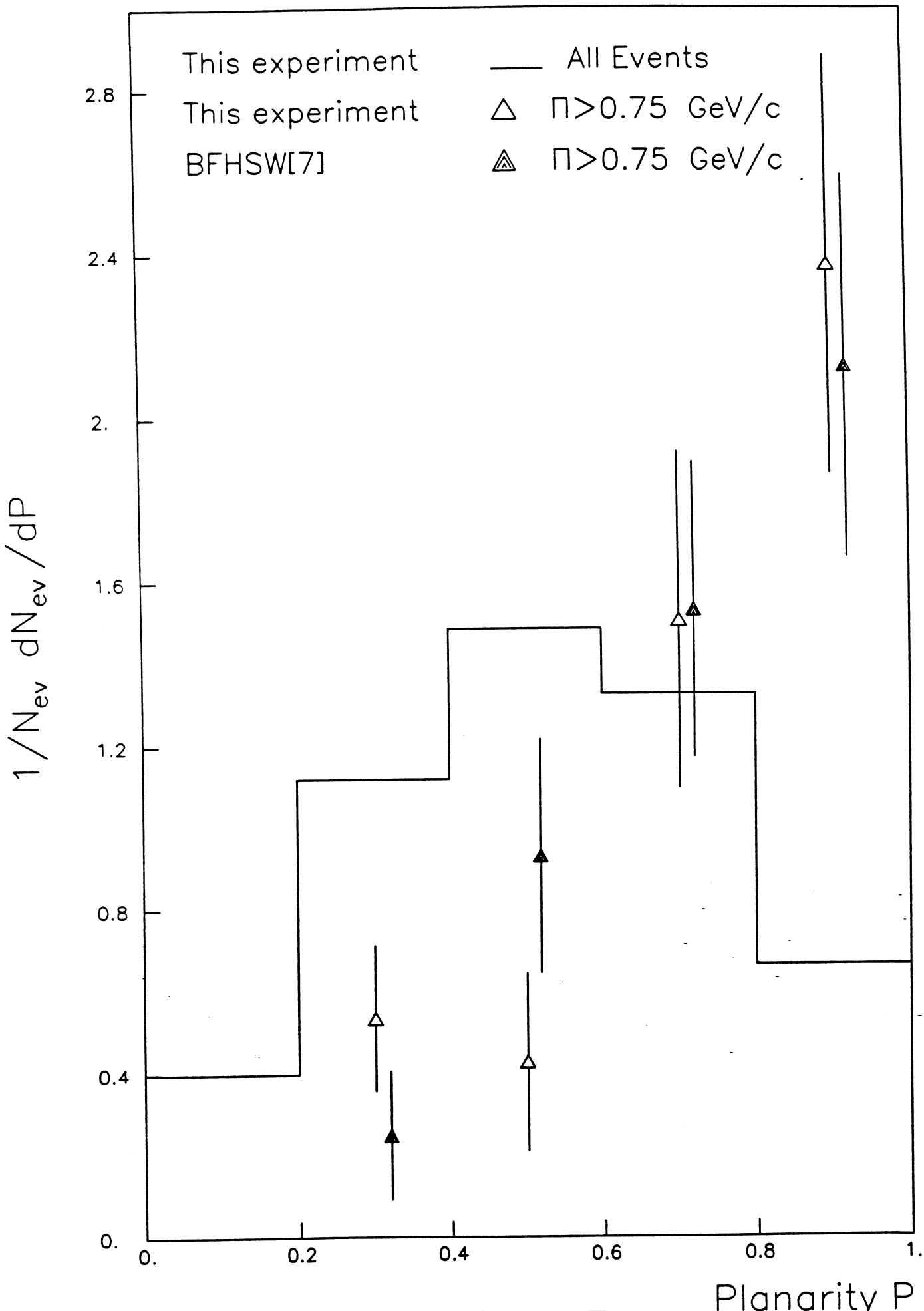
This experiment
All Events
This experiment
Π>0.75 GeV/c
BFHSW[7]
Π>0.75 GeV/c
2.8
2.4
2.
1.6
1.2
0.8
0.4
0.
0.
0.2
0.4
0.6
0.8
1.
1/N_ev dN_ev /dP
Planarity P

Figure 7

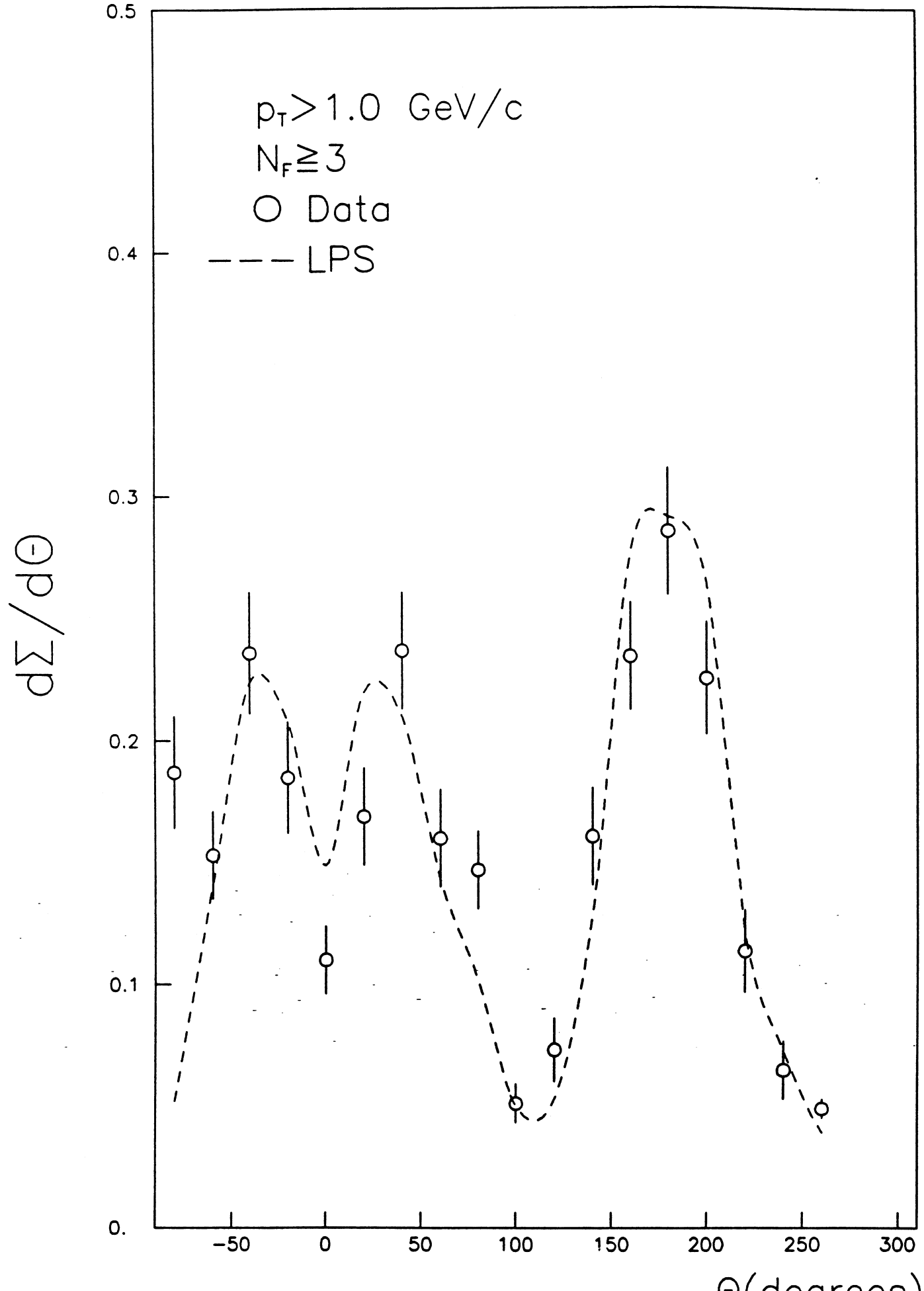
$p_T > 1.0$ GeV/c
$N_F \geq 3$
O Data
--- LPS
0.5
0.4
0.3
0.2
0.1
0.
$d\Sigma/d\Theta$
-50
0
50
100
150
200
250
300
Θ(degrees)

Figure 8

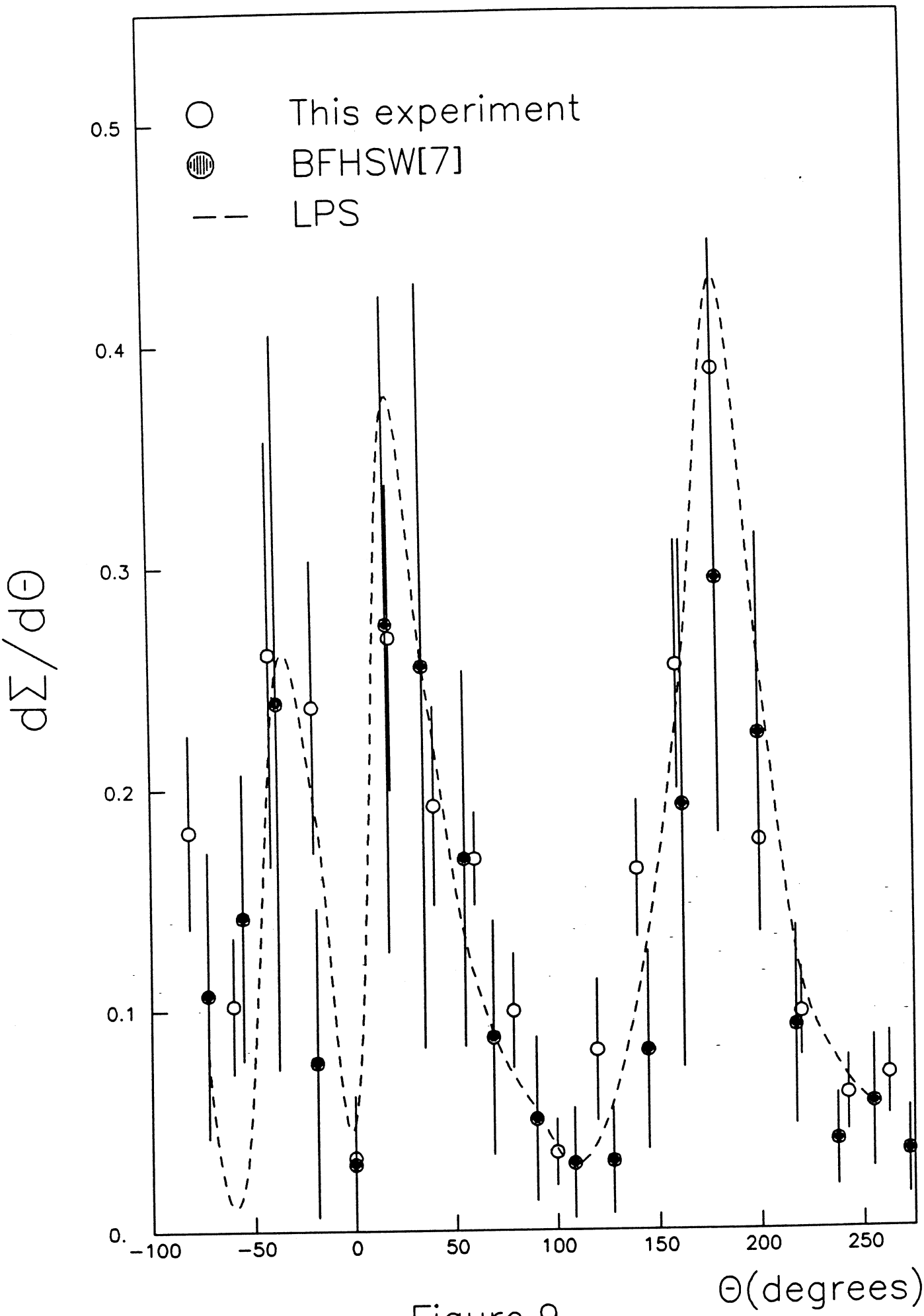
This experiment
BFHSW[7]
LPS
0.5
0.4
0.3
0.2
0.1
0.
dΣ/dΩ
−100
−50
0
50
100
150
200
250
Θ(degrees)

Fiaure 9